

INVITED REVIEW

Copolycarbonate optical films developed using birefringence dispersion control

Akihiko Uchiyama¹, Yuhei Ono¹, Yoshinori Ikeda¹, Hiroshi Shuto² and Kazuo Yahata²

A retardation film is a type of optical film that is widely used as a polarization transformation material to improve the image quality of flat panel displays (FPDs). One of the issues associated with retardation films has been the wide-banding of birefringence dispersion. A conventional optical design method that uses double-layered retardation films has been adopted to achieve wide-band properties. However, this conventional method has problems that have led to the demand for a single retardation film with wide-band birefringence properties. This situation motivated us to develop birefringence dispersion control (BDC) and to develop new polymers based on our novel molecular design. Wide-band characteristics are obtained using copolymers or miscible blends of polymers comprised of positive and negative anisotropic monomer units at specific volume fractions. The wide-band properties appear in a narrow range near the birefringence zero point, which is determined by the monomer volume fractions. The relationship between the orientation functions and birefringence dispersion is also clarified using theoretical studies, polarized IR and birefringence measurements. We have successfully industrialized a wide-band retardation film consisting of a newly developed copolycarbonate (co-PC) with a fluorene ring using the novel BDC theory. This film exhibits superior optical properties in FPDs.

Polymer Journal (2012) 44, 995–1008; doi:10.1038/pj.2012.52; published online 9 May 2012

Keywords: birefringence; dispersion; film; optical; polycarbonate; retardation

INTRODUCTION

Flat panel displays (FPDs), such as liquid crystal displays (LCDs) and organic light-emitting displays (OLEDs), have replaced conventional cathode ray tubes in televisions and personal computer monitors and have also helped create the new world of personal digital devices, such as mobile computers and smart phones. Optical retardation films, made of transparent polymers with refractive-index anisotropy, have been used to produce new high-quality displays that have high contrast and wide viewing-angle properties.^{1,2} The two most important functions of retardation films are to control the three-dimensional refractive indices and the wavelength dispersion of the birefringence.³

Retardation films can be divided broadly into two categories: a polymer-stretching type⁴ and a liquid crystal type⁵ that uses its spontaneous orientation. When referred to in this paper, the retardation film can be assumed to be of the former type unless otherwise specified.

Birefringence generated by polymer stretching causes optical retardation of the polarized incident beam, which is the film's most important function (Figure 1). Figure 1 describes an optical configuration at vertical incidence to the retardation film. The retardation film also has to control the polarization state of the oblique incident beam to improve the viewing-angle performance of LCDs. The viewing angle of the first generation of commercialized LCDs was

much narrower than the current generation. Many ideas have been developed to address this problem.^{5,6} The refractive-index anisotropy control of retardation films is one of the most effective solutions for improving performance and reducing costs and has become the standard means of improving the viewing angle.⁵

A second important development, which can address issues such as color dispersion and the contrast of FPDs, is the control of the birefringence dispersion on retardation films. Figure 2 shows a typical example of the effect of birefringence dispersion control (BDC) of the retardation film in a reflective LCD with a single polarizer. This figure illustrates how the film works to make a black state of an image. The retardation film described in Figure 2 is a quarter-wave plate that is required to switch between linear and circular polarization over a broad part of the visible light spectrum. Figure 3 shows the birefringence dispersion of conventional retardation films and the ideal dispersion when the anisotropy of the LC cell is neglected. The term 'wide-banding' in this paper refers to the process of having the birefringence dispersion curve approaching the ideal linear dispersion as much as possible. A 'wide-band retardation film' is defined in this study as a retardation film that exhibits these wide-banding characteristics. Figure 4 depicts schematically that the conventional retardation films that exhibit extremely non-ideal dispersion in LCDs (from Figure 2) do not succeed in obtaining low reflectance over a wider visible light range because the

¹New Business Development Group, Teijin Ltd., Tokyo, Japan and ²Teijin Chemicals Ltd., Ehime, Japan

Correspondence: Dr A Uchiyama, New Business Development Group, Teijin Ltd., Kasumigaseki Common Gate West Tower 2-1, Kasumigaseki 3-chome Chiyoda-ku, Tokyo 100-8585, Japan.

E-mail: a.uchiyama@teijin.co.jp

Received 31 January 2012; accepted 17 February 2012; published online 9 May 2012

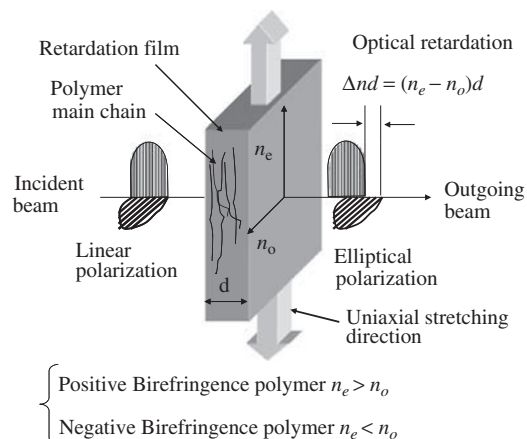


Figure 1 Conceptual view of a retardation film polarization conversion function.

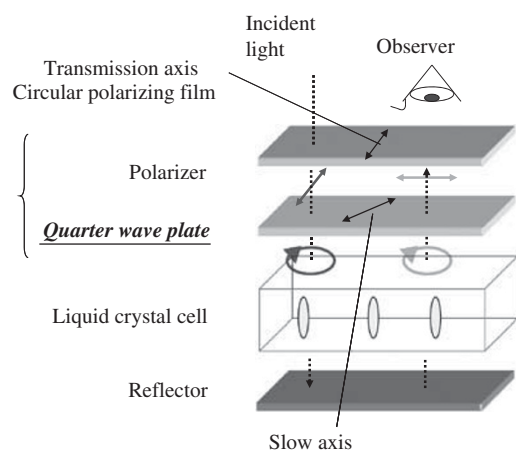


Figure 2 Polarization conversion mechanisms in the black state of a typical reflective LCD with a single polarizer. A full color version of this figure is available at *Polymer Journal* online.

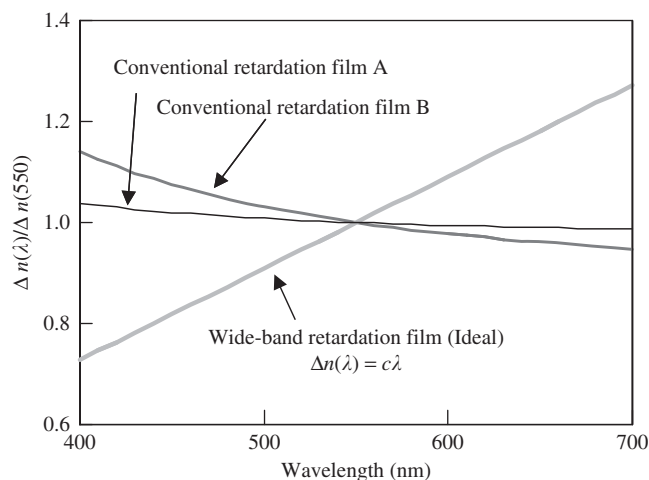


Figure 3 Birefringence dispersion of conventional and ideal wide-band retardation films. A full color version of this figure is available at *Polymer Journal* online.

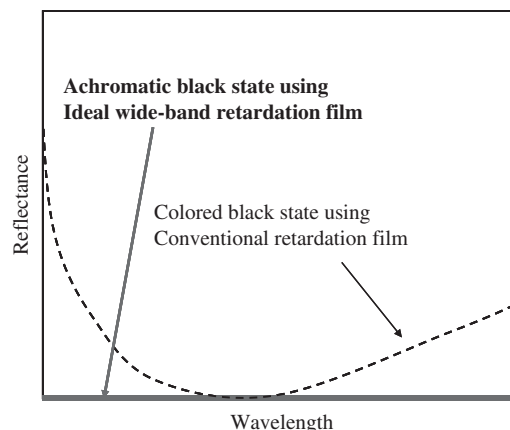


Figure 4 Conceptual view of two black state reflective spectra according to the difference in birefringence dispersion. A full color version of this figure is available at *Polymer Journal* online.

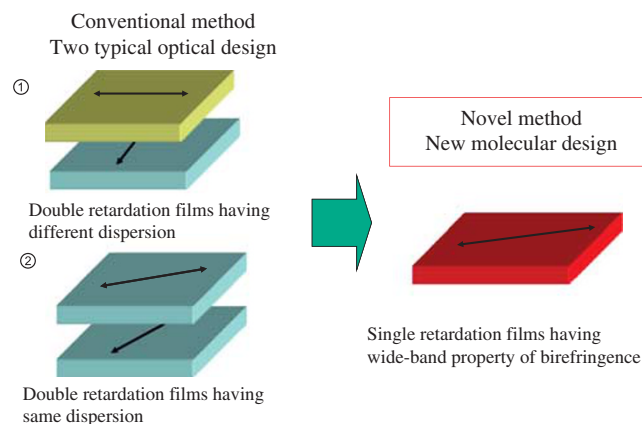


Figure 5 Conceptual differences between the new molecular and conventional optical design methods for wide-banding.

black state is not achromatic. This phenomenon occurs because the inadequate dispersion of the retardation value is quite different from the ideal dispersion at longer and shorter wavelength ranges. Wide-band retardation films (Figure 3) enable us to obtain low reflectance over a wide range of the visible spectrum. This example shows that BDC of retardation films is extremely important.

The birefringence dispersion of the retardation films was previously only controllable by conventional optical design methods using multi-layered retardation films with different optical parameters for each film.⁷ Multi-layered films were the only solution because there was no way of controlling the dispersion using a molecular design for a single retardation film. Figure 5 illustrates the conceptual difference between the two types of wide-band retardation films, one controlled by the new molecular design using a single polymer layer and the other by the conventional optical design using multiple layers. The new molecular design method to control the birefringence dispersion of polymers can solve many of the problems of the conventional multi-layered film, such as large film thicknesses, film processes of greater complexity and narrower viewing-angle properties. These improvements motivated our research to create novel molecular design methods and to develop new retardation films using them.^{8–11}

In this paper, we first describe the theory describing polymer birefringence and dispersion, which are extremely important concepts for explaining our new dispersion control that is based on molecular

design. Polymer birefringence has been thoroughly researched,^{12–16} but the method of controlling birefringence dispersion of polymers for wide-banding has not yet been explored. We therefore examined the theoretical behavior of our new BDC system and then experimentally validated the new BDC theory and the effects of orientation functions on birefringence dispersion. Finally, we introduced features of the newly developed wide-band retardation films made from copolycarbonate (co-PC).

THEORETICAL STUDY OF BDC

We first need to clarify the basic theoretical background to establish our BDC theory before we introduce our BDC theory.

Relationship between molecular orientation and birefringence dispersion

Amorphous polymers, such as polycarbonate (PC), cellulose ester, cycloolefin and acrylic resins, are the most widely used compounds for retardation films because they satisfy the basic optical requirements, including high transparency and extremely low polarization scattering in the visible spectrum. Therefore, this paper explores oriented amorphous polymers in its theoretical treatment of birefringence dispersion.

The relationship between molecular orientation and birefringence has previously been suggested using the statistical segment model,^{12–15} which is a hypothetical model that subdivides a linear polymer chain into cylindrical statistical segments having a vector \mathbf{n} in each segment. Assuming that \mathbf{n} has a statistical angular distribution, it can be described using equation (1):

$$\mathbf{n} = (\sin \theta \cos \phi, \sin \theta \sin \phi, \cos \theta) \quad (1)$$

The statistical average of \mathbf{n} is given by

$$\langle \mathbf{n} \rangle = \int \mathbf{n} p(\theta, \phi) d\Omega, \quad (2)$$

where $p(\theta, \phi)$ is the orientation distribution function. The molecular polarizability tensor of orientation birefringence in each segment is assumed to show uniaxial anisotropy because each segment in an amorphous polymer can rotate freely around the orientation axis and can allow the complex chemical structures of each segment to be averaged. Assuming that the molecular polarizability tensor can be described using equation (3), which is based on this segment model, then the polarizability tensor is described in the Cartesian coordinate system using equations (4) and (5). The relationship between the molecular polarizability of the single segment unit and that coordinate system is shown in Figure 6.¹⁶

$$\alpha = \begin{pmatrix} \alpha_{\perp} & 0 & 0 \\ 0 & \alpha_{\perp} & 0 \\ 0 & 0 & \alpha_{\parallel} \end{pmatrix} \quad (3)$$

$$\alpha = \begin{pmatrix} \alpha_{xx} & \alpha_{xy} & \alpha_{xz} \\ \alpha_{yx} & \alpha_{yy} & \alpha_{yz} \\ \alpha_{zx} & \alpha_{zy} & \alpha_{zz} \end{pmatrix} \quad (4)$$

$$\begin{aligned} \alpha_{xx} &= \alpha_{\perp} (\cos^2 \theta \cos^2 \phi + \sin^2 \phi) + \alpha_{\parallel} \sin^2 \theta \cos^2 \phi \\ \alpha_{yy} &= \alpha_{\perp} (\cos^2 \theta \sin^2 \phi + \cos^2 \phi) + \alpha_{\parallel} \sin^2 \theta \sin^2 \phi \\ \alpha_{zz} &= \alpha_{\perp} \sin^2 \theta + \alpha_{\parallel} \cos^2 \theta \\ \alpha_{xy} &= \alpha_{yx} = (\alpha_{\parallel} - \alpha_{\perp}) \sin^2 \theta \sin \phi \cos \phi \\ \alpha_{xz} &= \alpha_{zx} = (\alpha_{\parallel} - \alpha_{\perp}) \sin \theta \cos \theta \cos \phi \\ \alpha_{yz} &= \alpha_{zy} = (\alpha_{\parallel} - \alpha_{\perp}) \sin \theta \cos \theta \sin \phi \end{aligned} \quad (5)$$

Provided that the polymer has uniaxial anisotropy when the optical axis is z , the average polarizability tensor is described using

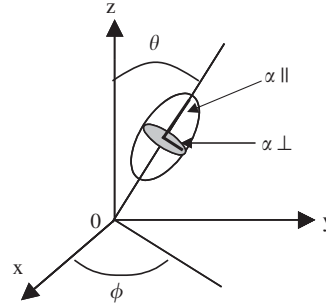


Figure 6 Definition of the molecular polarizability of a single segment unit in a rectangular coordinate system.

equation (6):

$$\begin{aligned} \langle \alpha_{xx} \rangle &= \langle \alpha_{yy} \rangle = \alpha_{\perp} \frac{(1 + \langle \cos^2 \theta \rangle)}{2} + \alpha_{\parallel} \frac{\langle \sin^2 \theta \rangle}{2} \\ \langle \alpha_{zz} \rangle &= \alpha_{\perp} \langle \sin^2 \theta \rangle + \alpha_{\parallel} \langle \cos^2 \theta \rangle \end{aligned} \quad (6)$$

The average polarizability tensor of biaxial anisotropy is similarly described by equation (7). In this case, the polarizability tensor of each segment unit and the total optical anisotropy are assumed to be uniaxial and biaxial, respectively.

$$\begin{aligned} \langle \alpha_{xx} \rangle &= \alpha_{\perp} (\langle \cos^2 \theta \cos^2 \phi \rangle + \langle \sin^2 \phi \rangle) + \alpha_{\parallel} \langle \sin^2 \theta \cos^2 \phi \rangle \\ \langle \alpha_{yy} \rangle &= \alpha_{\perp} (\langle \cos^2 \theta \sin^2 \phi \rangle + \langle \cos^2 \phi \rangle) + \alpha_{\parallel} \langle \sin^2 \theta \sin^2 \phi \rangle \\ \langle \alpha_{zz} \rangle &= \alpha_{\perp} \langle \sin^2 \theta \rangle + \alpha_{\parallel} \langle \cos^2 \theta \rangle \end{aligned} \quad (7)$$

The relationship between the molecular polarizability and the refractive index, which are microscopic and macroscopic physical quantities, respectively, is described by the Lorentz–Lorenz equation (8).

$$\frac{n_a^2 - 1}{n_a^2 + 2} = \frac{4\pi N}{3} \frac{\rho}{M} \langle \alpha \rangle \quad (8)$$

In the case of low birefringence, the birefringence is given by

$$\Delta n = n_z - n_y = \frac{2\pi}{9} \frac{(n_a^2 + 2)^2}{n_a} \frac{\rho N}{M} (\langle \alpha_{zz} \rangle - \langle \alpha_{yy} \rangle), \quad (9)$$

where n_a , ρ , M , N and $\langle \alpha \rangle$ are the average refractive index, the medium density, the molecular weight of the segment unit, Avogadro's number and the average polarizability of each segment unit, respectively. n_x , n_y and n_z are the three principal refractive indices in the direction of the x , y and z axes shown in Figure 6. In this paper, positively birefringent polymers are defined as oriented polymers in which the direction of the largest refractive index is parallel to the main uniaxial stretching direction and negatively birefringent polymers are oriented polymers in which the direction of the largest refractive index is perpendicular to the main uniaxial stretching direction (see Figure 1). n_e and n_o are extraordinary and ordinary refractive indices, respectively, which are defined as $n_x = n_y = n_o$ and $n_z = n_e$ using the coordinates used in Figure 6.

In uniaxial and biaxial films, birefringence values in the yz plane are described using Equations (10) and (11), respectively. The molecular polarizabilities and average refractive indices are functions of the wavelength, but the terms of orientation distribution are not

functions of the wavelength in those birefringence equations.

$$\Delta n = \frac{3\langle \cos^2 \theta \rangle - 1}{2} \frac{4\pi}{9} \frac{(n_a^2 + 2)^2}{n_a} \frac{\rho N}{M} (\alpha_{\parallel} - \alpha_{\perp}) \quad (10)$$

$$\Delta n = (\langle \cos^2 \theta \rangle - \langle \sin^2 \theta \sin^2 \phi \rangle) \frac{4\pi}{9} \frac{(n_a^2 + 2)^2}{n_a} \frac{\rho N}{M} (\alpha_{\parallel} - \alpha_{\perp}) \quad (11)$$

The terms $(3\langle \cos^2 \theta \rangle - 1)/2$ and $\langle \cos^2 \theta \rangle - \langle \sin^2 \theta \sin^2 \phi \rangle$ expressing the molecular orientation are the orientation functions, f , whereas the other terms are defined as the intrinsic birefringence Δn^0 .¹⁷ Therefore, the birefringence in both uniaxial and biaxial films is written as

$$\Delta n(\lambda) = f \Delta n^0(\lambda). \quad (12)$$

For instance, a functional group in a polymer structure can be assumed to be a segment unit of that segment model. However, to construct a practical and simple molecular design, the monomer unit of the polymer should be defined as the segment unit. Therefore, the monomer unit is used as the segment unit of the segment model in this paper.

The normalized birefringence dispersion of a homopolymer should be constant, as shown in equation (13) (which is derived from equation (12)).

$$\frac{\Delta n(\lambda)}{\Delta n(\lambda_0)} = \frac{\Delta n^0(\lambda)}{\Delta n^0(\lambda_0)} = C \quad (13)$$

Equation (13) is theoretically valid under the assumption that the intrinsic birefringence of a homopolymer is constant with respect to changes in molecular orientation. This conclusion is supported by the result that the normalized birefringence dispersion of Bisphenol A (BPA) homo-PC is constant and shows no dependency on molecular orientation.¹⁸ Equation (13) also shows the dispersion of the molecular anisotropic polarizability of a monomer unit in the homopolymer, and this equation is extremely useful for obtaining a microscopic physical value using a macroscopic birefringence measurement. Therefore, the normalized dispersion is used as an expression of birefringence dispersion in this paper. The birefringence at 550 nm is used for the normalization procedure because it lies in the center of the visible spectrum (400–700 nm) that is used in FPDs.

Birefringence dispersion of a multi-component polymer system

In our new molecular design, a multi-component polymer system, such as a copolymer or a blend polymer, is employed to control birefringence dispersion. The total birefringence Δn of the multi-component system is given by¹⁵

$$\Delta n = \sum_i v_i \Delta n_i + \sum_i v_i \Delta n_i^d + \Delta n^f, \quad (14)$$

where the first, second and third terms are the static birefringence of molecular orientation, dynamically stress-induced birefringence by elastic deformation and the form birefringence, respectively. v_i , Δn_i and Δn_i^d represent the volume fraction, the orientation birefringence and the stress-induced birefringence of the i -th component, respectively. The second term is almost negligible within the normal operating environment of retardation films. The form birefringence is also negligible because we do not use the form birefringence effect for our new design. Therefore, equation (14) can be transformed to

equation (15).

$$\Delta n = \sum_i v_i \Delta n_i \quad (15)$$

Equation (15) is also derived from the Lorentz–Lorenz equation (16) for multi-component systems (equations (8) and (9)).¹⁹

$$\frac{n_a^2 - 1}{n_a^2 + 2} = \sum_i v_i \frac{n_i^2 - 1}{n_i^2 + 2} \quad (16)$$

n_a and n_i are the average refractive index and the refractive index of the i -th component, respectively. This equation is valid under the assumption that the refractive index of each component does not change in the multi-component system. Therefore, the same assumption is necessary for equation (15). This assumption is used later to discuss BDC using the multi-component polymer system.

Equation (13) for the multi-component system can be transformed to equation (17).

$$\frac{\Delta n(\lambda)}{\Delta n(\lambda_0)} = \frac{\sum_i v_i f_i \Delta n_i^0(\lambda)}{\sum_i v_i f_i \Delta n_i^0(\lambda_0)} \quad (17)$$

If each orientation function for the monomer units is the same, then f can be neglected and equation (17) can be rewritten as equation (18).

$$\frac{\Delta n(\lambda)}{\Delta n(\lambda_0)} = \frac{\sum_i v_i \Delta n_i^0(\lambda)}{\sum_i v_i \Delta n_i^0(\lambda_0)} \quad (18)$$

Equation (18) should be constant under the assumption that each intrinsic birefringence does not vary and that the orientation functions of each segment unit are the same for any stretching parameters. Equation (18) also predicts that the birefringence dispersion should only depend on the volume fractions of the monomer units, provided the assumption is valid.

Birefringence dispersion of conventional polymers and the necessary condition for the wide-band property

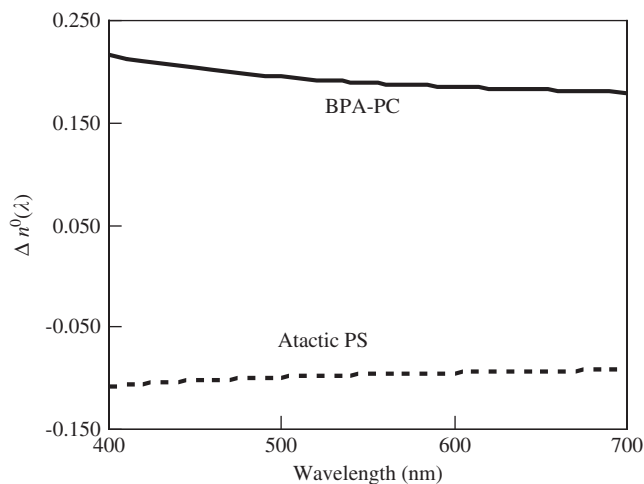
Figure 7 show the intrinsic birefringence dispersion of uniaxially oriented films consisting of BPA-PC¹⁸ and atactic polystyrene (PS),^{20,21} respectively. Equation (13) was previously verified to be valid for both of these homopolymers.^{19–21} Therefore, the intrinsic birefringence dispersions are same as the birefringence dispersions for the homopolymers. These homopolymers are typical examples of materials that have only narrow-band birefringent properties. These positive and negative birefringence homopolymers also show negative and positive slopes, respectively (see Figure 7). The relationships between birefringence and the slopes of conventional polymers are summarized in Table 1.

The conditions required for wide-band properties are listed in Table 2. The absolute values of birefringence must increase with increasing wavelengths in the visible range for wide-banding. Therefore, both the birefringence and the slope of wide-band retardation films must be either positive or negative. These conditions are valid for both uniaxial and biaxial films.

The classic Lorentz model of dielectric dispersion is simple, but it can qualitatively explain the birefringence dispersion of conventional polymers in Table 1. Media with higher refractive indexes have lower natural angular frequencies using this model. The natural angular frequency is related to the wavelength of maximal absorption. Therefore, if a material has a lower natural angular frequency, then the wavelength of maximal absorption shifts to longer wavelengths. This model leads to the conclusion that media with higher refractive

Table 1 The relationships between the birefringence and the slopes of conventional retardation films

	Birefringence (Δn)	Slope ($d\Delta n/d\lambda$)
Conventional retardation film 1	Positive	Negative
Conventional retardation film 2	Negative	Positive


Figure 7 Intrinsic birefringence dispersion of BPA-PC and atactic PS.

indexes will produce greater absolute values of their slope in the visible spectrum. The relationship between extraordinary and ordinary refractive indices in positive birefringence polymers is $n_e > n_o$; according to the Lorentz model, the birefringence slope should therefore be negative. This conclusion is supported by many experimental results, including those obtained with the BPA-PC and PS homopolymers shown in Figure 7. These results also indicate that a new molecular design must be established to control the wavelength dispersion for wide-banding.

New molecular design concept for the control of birefringence dispersion

As mentioned above, controlling birefringence dispersion and making it wide-banding is difficult using only a homopolymer. We have paid much attention to the large differences in slopes between birefringence-positive and -negative polymers. First, to simplify the discussion, we use equation (15) to examine the necessary conditions for two-component polymer systems consisting of a positive and negative birefringence unit. The equations that describe the necessary conditions for a wide-band retardation film (listed in Table 2) are written as

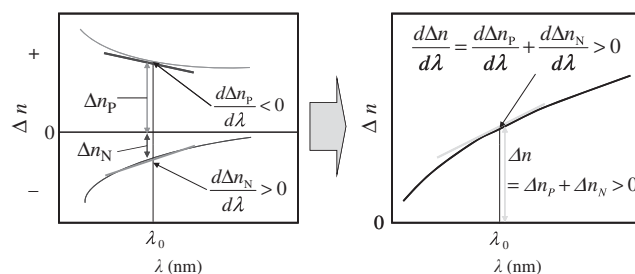
$$\Delta n = \Delta n_P + \Delta n_N > 0 \quad (19)$$

$$\frac{d\Delta n}{d\lambda} = \frac{d\Delta n_P}{d\lambda} + \frac{d\Delta n_N}{d\lambda} > 0, \quad (20)$$

where Δn_P and Δn_N are the total birefringence of the positive and negative segment units in the two-component polymer system, respectively. The meaning of equations (19) and (20) is illustrated in Figure 8. As shown in Figure 8, the sum of positive and negative birefringence must increase with increasing wavelengths to satisfy the above necessary conditions. The other necessary condition for a wide-

Table 2 Necessary conditions for wide-band retardation films

	Birefringence (Δn)	Slope ($d\Delta n/d\lambda$)
Wide-band retardation film 1	Positive	Positive
Wide-band retardation film 2	Negative	Negative


Figure 8 Basic concept of BDC using birefringence-positive and -negative segment units. A full color version of this figure is available at *Polymer Journal* online.

band retardation film is expressed by equations (21) and (22).

$$\Delta n = \Delta n_P + \Delta n_N < 0 \quad (21)$$

$$\frac{d\Delta n}{d\lambda} = \frac{d\Delta n_P}{d\lambda} + \frac{d\Delta n_N}{d\lambda} < 0 \quad (22)$$

All of these necessary conditions are generalized using equation (15) for the multi-component polymer system, as follows:

$$\Delta n = \sum_i v_i \Delta n_i > 0 \text{ and } \frac{d\Delta n}{d\lambda} = \sum_i v_i \frac{d\Delta n_i}{d\lambda} > 0 \quad (23)$$

or

$$\Delta n = \sum_i v_i \Delta n_i < 0 \text{ and } \frac{d\Delta n}{d\lambda} = \sum_i v_i \frac{d\Delta n_i}{d\lambda} < 0. \quad (24)$$

These equations are valid under the assumption that the birefringence change induced by the interactions between each component and the form birefringence are negligible.

Equations (23) and (24) are established using the birefringence equations for each component, which are macroscopic physical properties. In the next step, we examine the relationship between the necessary conditions and the molecular polarizabilities of monomer units to choose best the molecular design of each monomer unit. From equations (12) and (15), the total birefringence of a multi-component polymer system can be written as

$$\Delta n = \sum_i v_i f_i \Delta n_i^0(\lambda). \quad (25)$$

This equation expresses the relationships between the macroscopic birefringence Δn and the intrinsic birefringence, which is composed of the sum of the microscopic molecular anisotropic polarizabilities of the monomer units. Therefore, to satisfy equations (23) or (24) in the multi-component polymer system, the polymer should be designed using monomer units with positive and negative anisotropies of

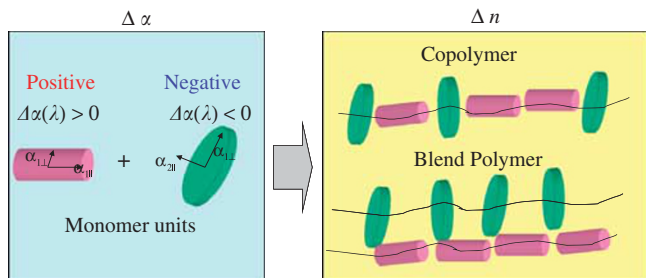


Figure 9 Polymer design concept for wide-band retardation films.

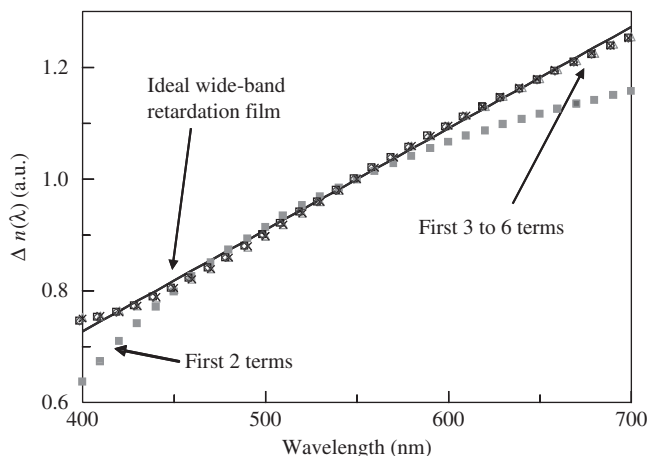


Figure 10 Curve fitting to ideal wide-band retardation films using Cauchy's equations with different term numbers. A full color version of this figure is available at *Polymer Journal* online.

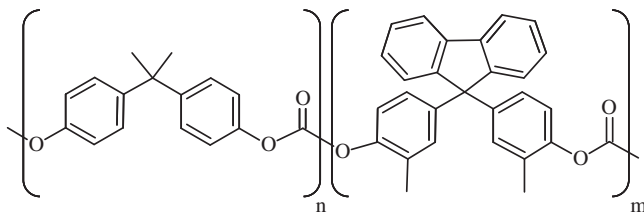


Figure 11 Polymer structure of copolycarbonate(BPA/BMPF).

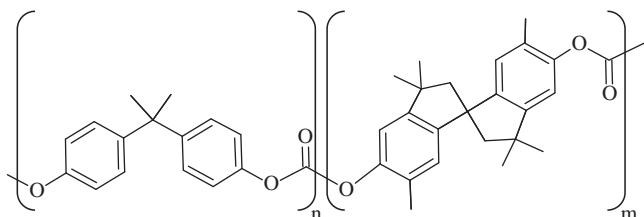


Figure 12 Polymer structure of co-PC(BPA/SPI).

molecular polarizability. equations (23) and (24) are transformed to

$$\Delta n = \sum_i v_i f_i \Delta n_i^0(\lambda) > 0 \text{ and } \frac{d\Delta n}{d\lambda} = \sum_i v_i f_i \frac{d\Delta n_i^0}{d\lambda} > 0 \quad (26)$$

and

$$\Delta n = \sum_i v_i f_i \Delta n_i^0(\lambda) < 0 \text{ and } \frac{d\Delta n}{d\lambda} = \sum_i v_i f_i \frac{d\Delta n_i^0}{d\lambda} < 0, \quad (27)$$

respectively.

A copolymer or a miscible polymer blend can be used to create polymers with positive and negative anisotropic monomer units. The polymer design concept is illustrated in Figure 9. These polymers must satisfy Equations (26) or (27) to obtain wide-banding properties. The resulting polymers make up our new design concept of BDC for wide-band retardation films.

Curve-fitting equation for birefringence dispersion

Cauchy's equation (equation (28)) is generally used to describe the relationship between birefringence and the wavelength of light.

$$\Delta n = A + \frac{B}{\lambda^2} + \frac{C}{\lambda^4} + \dots \quad (28)$$

This equation is derived from the classic Lorentz model of dielectric dispersion that expresses resonance dispersion although neglecting quantum effects. It is well known that this empirical equation is fitted with the polymer birefringence dispersion that birefringence decreases with increasing wavelengths.²² However, there have been no attempts to examine whether the equation applies to birefringence dispersions that increase with increasing wavelengths of light. Figure 10 shows the fitting results for an ideal wide-band dispersion to ascertain the necessary parameter values for equation (28). Using the first three terms of Cauchy's equation is sufficient to express ideal dispersion, as shown in Figure 10. Therefore, we use this equation up to the third term to fit the birefringence dispersion curve. In this paper, the birefringence slopes are calculated at 550 nm using this equation.

EXPERIMENTAL PROCEDURE

Polymerization

Co-PC consists of two kinds of monomer units. Aromatic PCs containing fluorene side chains were synthesized from 2,2-bis(4-hydroxyphenyl)propane (BPA), 9,9-bis(4-hydroxy-3-methyl phenyl) fluorene (BMPF) and phosgene by interfacial polycondensation for use in experiments aimed at verifying the BDC theory described above. BPA homo-PC is a positive birefringence polymer and BMPF homo-PC is a negative birefringence polymer. The copolymer ratio was controlled by changing the feed ratio of BPA and BMPF. The polymer structure is described in Figure 11. The details of the polymerization conditions used have been described in our previous report.²³

Co-PCs consisting of BPA and 3,3,6,3',3',6'-hexamethyl-1,1'-spirobiindane-5,5'-diol (SPI) monomer units were synthesized using the same method. The SPI homopolymer used exhibits negative birefringence, and its structure is illustrated in Figure 12.

Miscible blend polymers consisted of two kinds of monomer units. Atactic polystyrene ($\bar{M}_n = 90\,900$, $\bar{M}_w = 243\,000$, PS) and poly(2,6-dimethyl 1,4-phenylene oxide) ($\bar{M}_n = 6200$, $\bar{M}_w = 42\,500$, PPO) were purchased from Aldrich (Tokyo, Japan). The molecular weights were estimated using gel permeation chromatography.

Polymer characterization

The glass transition temperature was obtained using a TA Instruments DSC 2920 differential scanning calorimeter at a heating rate of $20\text{ }^\circ\text{C min}^{-1}$. The intrinsic viscosities of the co-PCs were measured using an Ubbelohde capillary

viscometer. The monomer ratios and copolymer sequences of the co-PCs were analyzed using $^1\text{H-NMR}$ and $^{13}\text{C-NMR}$, respectively.

Film preparation

The film samples were prepared by solvent casting. The BPA and BMPF co-PCs with molar fractions of BMPF units ranging from 0 to 0.85 were dissolved in dichloromethane (18–20 wt%) and coated onto glass substrates.^{23,24} The BMPF homopolymer was dissolved in Chloroform (22 wt%). Co-PCs containing SPI monomer units were also dissolved in dichloromethane (18–20 wt%) and coated onto glass substrates. After film casting, the films were dried at 40 °C for 10 h and peeled from the glass substrate. The films were further dried and annealed at a temperature 10 °C higher than the glass transition temperature (T_g) of the material for 1 h to remove the solvents and alleviate internal stresses. The film thicknesses were measured using an Anritsu K351C electronic micrometer and ranged from 20 to 200 μm .

A blend of PS and PPO and a PPO homopolymer were dissolved in chloroform (20 wt%) and coated onto glass substrates.^{20,21} The PS homopolymer was dissolved in dichloromethane (20 wt%). After film casting, the films were dried at 30 °C for 10 h and peeled from the glass substrate. The films were further dried and annealed for 12 h at a temperature 10 °C higher than the glass transition temperature of the material to remove the solvents and alleviate the internal stresses. Their thicknesses ranged from 40 to 100 μm .

All these films were optically isotropic. The uniaxially oriented films used to measure the intrinsic birefringence and birefringence dispersion values were prepared as follows. Each isotropic film was fixed in a uniaxial orientation device placed in an oven at the experimental temperature. After 5 min, when the film had reached the equilibrium temperature, it was stretched to a set position at 120 mm min^{-1} and was immediately cooled to room temperature.

Birefringence and polarized IR

A spectro-ellipsometer (JASCO M150) equipped with a monochromator, a photoelastic modulator and a dual lock-in amplifier was employed for measuring birefringence, intrinsic birefringence and birefringence dispersion. The measurement principle behind birefringence is based on polarization-modulated transmission spectro-ellipsometry.²⁵ The wavelengths used for intrinsic birefringence and birefringence dispersion measurements ranged from 400 to 700 nm.

The birefringence slopes at 550 nm were obtained from the fitting curves using Cauchy's equation (28).

The birefringence of uniaxially oriented amorphous polymer film samples was measured. The orientation functions are expressed by

$$f = \frac{3 \langle \cos^2 \theta \rangle - 1}{2} \quad (29)$$

This orientation function is evaluated from the infrared dichroic ratio $D = A_{\parallel}/A_{\perp}$ of any absorption band; A_{\parallel} and A_{\perp} are the absorbances parallel and perpendicular to the stretching direction, respectively. The orientation function, f , is written as

$$f = \frac{(D-1)(2 \cot^2 \alpha + 2)}{(D+2)(2 \cot^2 \alpha - 1)} \quad (30)$$

Where, α is the angle between the transition moment vector of the absorbing group and the axis. Equation (30) allows f to be determined by measuring the value for D of the IR absorption with a known α . The dichroic function is described as $(D-1)/(D+2)$. The IR spectra of uniaxially oriented films were obtained using a Shimadzu FTIR-8100M Fourier transform infrared (FTIR) spectrometer.²⁶ All spectra were recorded at a resolution of 2 cm^{-1} using 200 scans. The assignment of the infrared dichroic absorption bands and other details have been published in our previous reports.^{20,21,23,24}

Durability evaluation

The stability of the retardation and birefringence dispersion were tested at 80 °C for 1000 h in an Espec thermostat chamber.

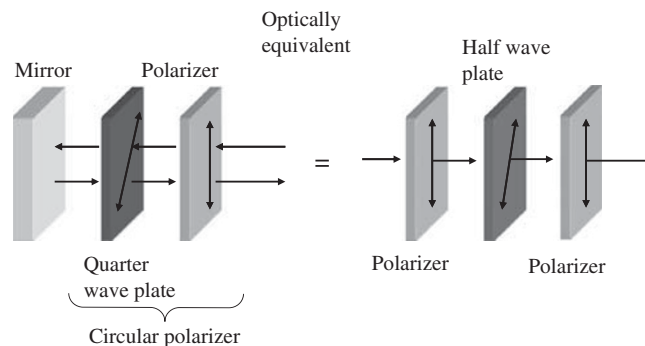


Figure 13 Optically equivalent model measuring the wide-band properties of circular polarizers. A full color version of this figure is available at *Polymer Journal* online.

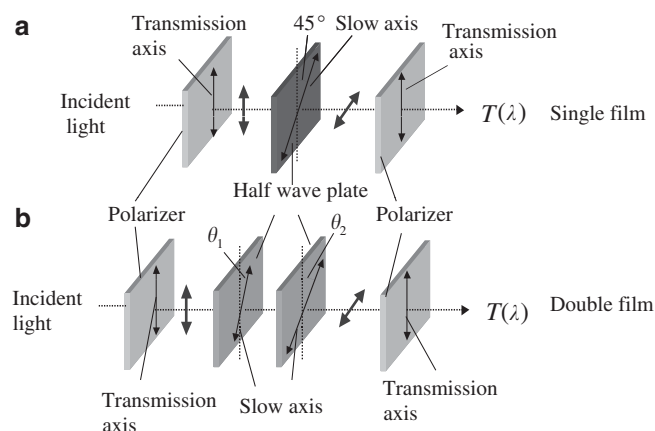


Figure 14 Optical configurations for transmission spectral measurements of the optically equivalent models in Figure 13. A full color version of this figure is available at *Polymer Journal* online.

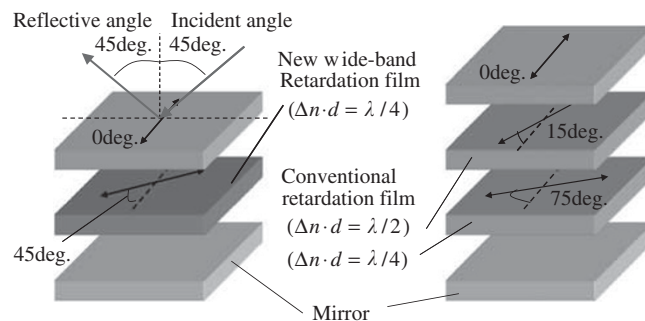


Figure 15 Optical configurations for measurements of reflective viewing-angle properties. A full color version of this figure is available at *Polymer Journal* online.

Evaluation of the optical performance of wide-band retardation films

The new single wide-band retardation film and the conventional films were evaluated using wide-band quarter-wave plates for circular polarizing films. The film with wide-banding properties was prepared from the co-PC synthesized from BPA and BMPF ($v_p = 0.24$). The conventional film samples were prepared from homo- BPA-PC polymer. We evaluated the wide-band properties of the circular polarizing films using their reflective spectrums and viewing angle properties. The retardation films used in this experiment were optically uniaxial. An equivalent transmissive optical system based on the concept illustrated in Figure 13 rather than a reflective evaluation system was employed to avoid the surface reflection of circular polarizing films in the

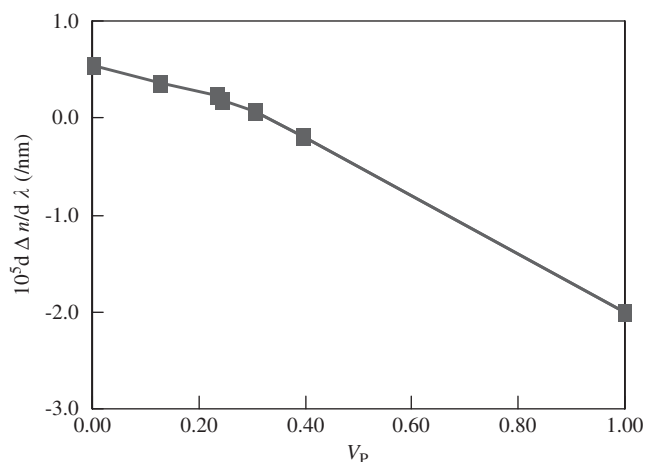


Figure 16 Birefringence slopes of the uniaxially oriented co-PC (BPA/BMPF) films as a function of the BPA volume fraction. The film samples were stretched at $T_g + 5$ degree C and a stretching ratio of 2.1. A full color version of this figure is available at *Polymer Journal* online.

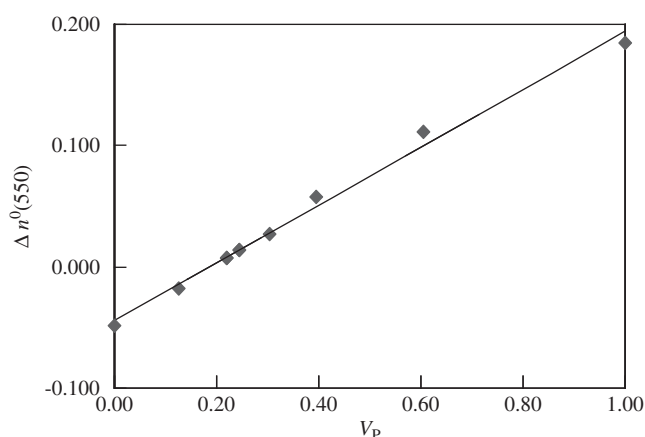


Figure 17 Intrinsic birefringence of co-PCs (BPA/BMPF) as a function of the BPA volume fraction. The solid line represents a least-squares linear plot. A full color version of this figure is available at *Polymer Journal* online.

evaluation. The optical configurations of single and double-layered retardation films are shown in Figure 14. Visible transmission spectra were recorded using a Hitachi U-4000 spectrometer. The viewing angle properties of the reflectance were recorded using an Otsuka electronics LCD-5100 evaluation system, the optical configuration of which is described in Figure 15. The circular polarizing film was attached to an aluminum reflector using a transparent adhesive agent. The light intensity of the viewing angle measurement was evaluated using Y values of the CIE 1931 XYZ color space.⁹

RESULTS AND DISCUSSION

Verifying the BDC theory using a two-component polymer system

We first examined the BDC using the synthesized co-PC consisting of BPA and BMPF monomer units. Figure 16 shows the relationship between the volume fraction of positive monomer units (BPA) and the birefringence slopes at 550 nm. Figure 17 illustrates the intrinsic birefringence dependence on the volume fraction of positive monomer units. The intrinsic birefringence is zero at $v_p = 0.18$; therefore, the birefringence is always positive at $v_p > 0.18$. The slope is also positive at $v_p < 0.31$. It should be noted that these polymer films satisfy equation (26), one of the two necessary conditions for wide-

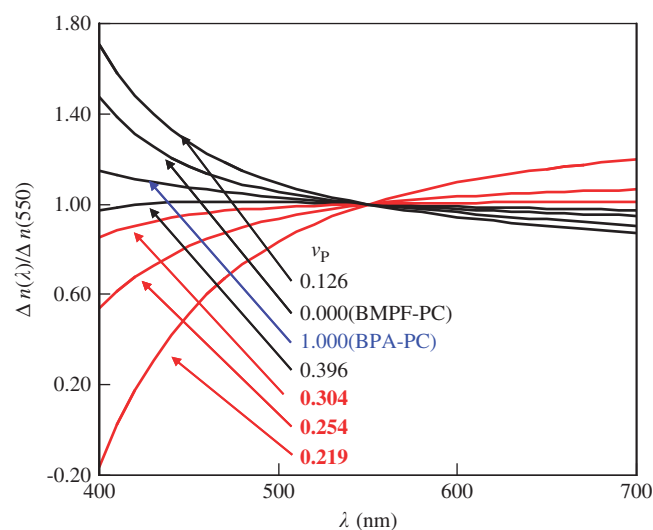


Figure 18 Normalized birefringence dispersion of the uniaxially oriented co-PC (BPA/BMPF) films as a function of the BPA volume fraction.

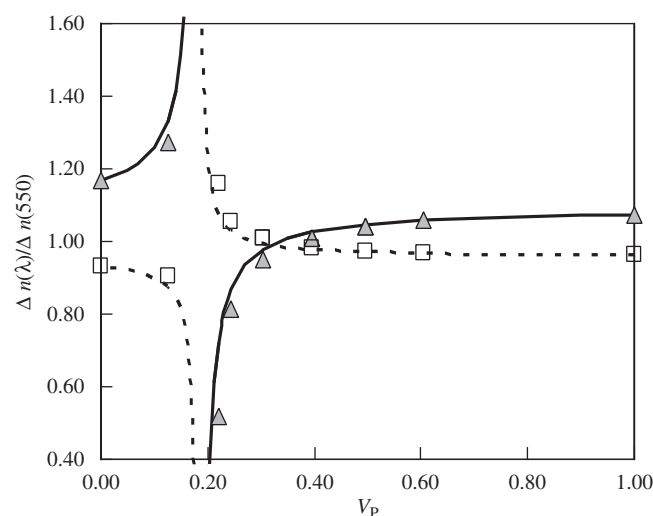


Figure 19 Normalized birefringence dispersion of the uniaxially oriented co-PC (BPA/BMPF) films stretched at $T_g + 5$ degree C and a draw ratio of 2.1 as a function of the BPA volume fraction. The triangles and squares indicate experimental results measured at $\lambda = 450$ and 650 nm, respectively. The thin and broken lines show the theoretical results calculated for $\lambda = 450$ and 650 nm, respectively, using Equation (18) and the parameters listed in Table 3. A full color version of this figure is available at *Polymer Journal* online.

banding, when the volume fraction of positive monomer units is in the range:

$$0.18 < v_p < 0.31. \quad (31)$$

Figure 18 demonstrates the normalized birefringence dispersion based on the volume fraction v_p . Figure 18 demonstrates that co-PC retardation films with volume fractions satisfying Equation (31) exhibit wide-band properties. These results support our BDC theory.

Figure 19 shows the relationship between the volume fraction of positive monomer units and the normalized birefringence dispersion. The dots and lines represent the experimental and calculated results, respectively. Importantly, the calculated values are consistent with the experimental results. These theoretical values were calculated using

Equation (18) and the parameters of the homo- BPA and BMPF polymers were listed in Table 3. This consistency demonstrates that this copolymer system obeys equation (18) for the multi-component system, indicating that the form birefringence and the stress-induced birefringence are negligible, whereas the intrinsic birefringence of each component is constant even in a multi-component system. These results support the validity of our BDC theory.

The BMPF homopolymer exhibits negative birefringence (Figure 17). Figure 20 presents the polarized IR spectra in the range of 1350–1470 cm^{-1} for the uniaxially oriented BPA and BMPF co-PC films. The absorbance at 1449 cm^{-1} was assigned to various combinations of CC stretching and CH in-plane bending vibrations in the fluorene ring. The perpendicular absorbance at 1449 cm^{-1} is greater than the parallel absorbance.²² The fluorene ring is also assumed to have large molecular polarizability anisotropy. Therefore, the negative birefringence can be explained by the fluorene plane being perpendicular to the polymer chain axis.

Figure 21 illustrates the birefringence dispersion of the BPA and SPI co-PC film, which exhibited wide-band birefringence properties, negative slope and negative birefringence values, which satisfy the necessary conditions expressed in equation (27).

It should be noted that a wide-band retardation film can experimentally satisfy either equation (26) or equation (27). In this paper, we demonstrate that two types of wide-band retardation films exist, as defined by those two equations. Table 4 presents the birefringence dispersions of homopolymers consisting of each monomer component of the two co-PC types. Table 4 also indicates that the magnitude of the correlation of the birefringence dispersion of the positive and negative birefringence monomer units decides the type of wide-band retardation film (1 or 2) (Table 2). This result can be theoretically explained by equation (17).

Necessary and sufficient conditions for the industrialization of new wide-band retardation films

Birefringence dispersion is one of the most important specifications for wide-band retardation films. However, in addition to BDC, many other required specifications exist for polymers used in retardation films; these specifications include the necessary birefringence values linked to the polymer orientation and the intrinsic birefringence, thermal stability and mechanical properties. Furthermore, the retardation films require sophisticated optical qualities, such as optical uniformity and decreasing defects, based on chemical and physical gels. We have examined many polymers to obtain wide-band retardation films that satisfy all the required specifications. One of the best materials provided by our screen is an aromatic co-PC consisting of BPA and BMPF monomer units that is introduced in this paper. The main reasons for the conclusion are as follows:²⁷

- (1) Wide-band birefringence dispersion
- (2) Sufficient birefringence values
- (3) Stability of the birefringence dispersion
- (4) Durability

The first property has already been discussed, and the third and fourth properties are discussed in the following sections. The second property, which is discussed in this section, requires that the polymers used for retardation films generate sufficiently large birefringence. Wide-band retardation films are mostly used as quarter-wave plates in FPDs with a required retardation of approximately 140 nm at a measurement wavelength of 550 nm. The film thickness should be <80 μm because of the thickness limitations regarding the thinner

Table 3 Optical parameters for calculating the birefringence dispersion

	Positive unit (BPA homopolymer)	Negative unit (BMPF homopolymer)
$\Delta n^0(550)$	0.200	-0.045
$\Delta n^0(450)/\Delta n^0(550)$	1.074	1.167
$\Delta n^0(650)/\Delta n^0(550)$	0.962	0.932

Abbreviations: BMPF, 9,9-bis(4-hydroxy-3-methyl phenyl)fluorene; BPA, bisphenol A. The values were obtained experimentally using homopolymers.

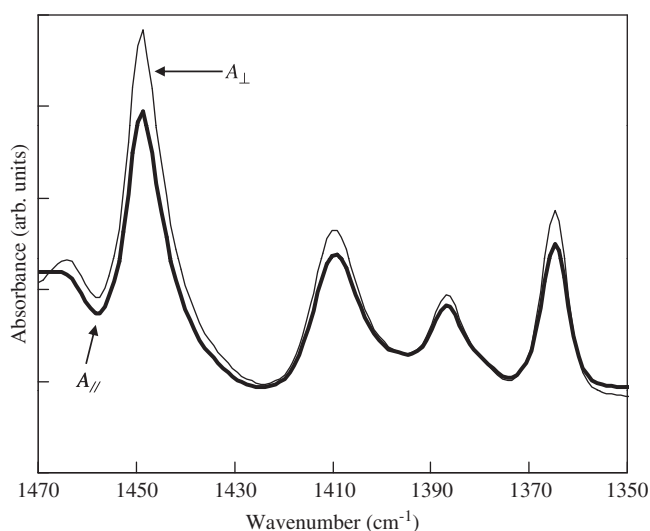


Figure 20 Polarized IR spectra in the range 1350–1470 cm^{-1} for the uniaxially oriented consisting of co-PC (BPA/BMPF) film (BPA = 70.0 mol%).

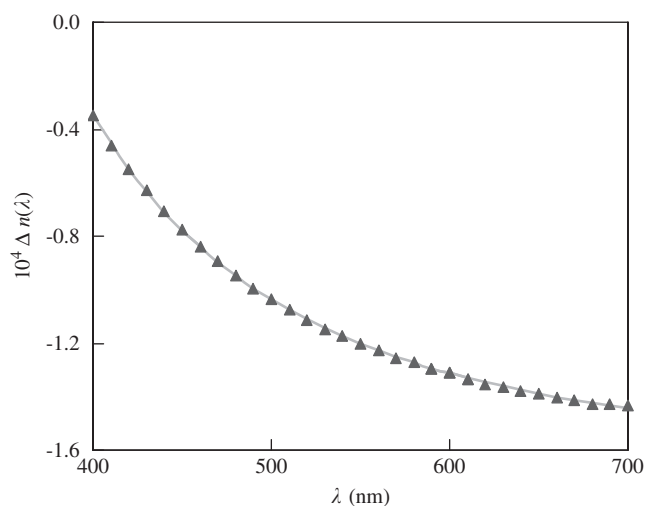
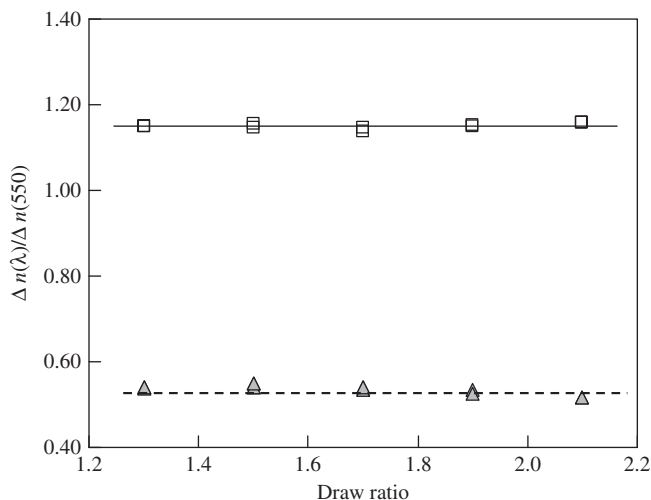


Figure 21 Birefringence dispersion of the uniaxially oriented co-PC (BPA/SPI) film (BPA = 22.4 mol%). The film was stretched at 230 °C and a draw ratio of 1.9. The triangles and solid line show the experimental results and the curve fitted using equation (28). A full color version of this figure is available at *Polymer Journal* online.

Table 4 Normalized birefringence dispersion of the uniaxially oriented homopolymer films, stretched at $T_g + 5$ degree C and using a draw ratio of 2.1

	BPA-PC	BMPF-PC	SPI-PC
$\Delta n(450)/\Delta n(550)$	1.074	1.167	1.046
$\Delta n(650)/\Delta n(550)$	0.962	0.932	0.971

Abbreviations: BMPF, 9,9-bis(4-hydroxy-3-methyl phenyl)fluorine; BPA, bisphenol A; SPI, 3,3,6,3',3',6'-hexamethyl-1,1'-spirobiindane-5,5'-diol.

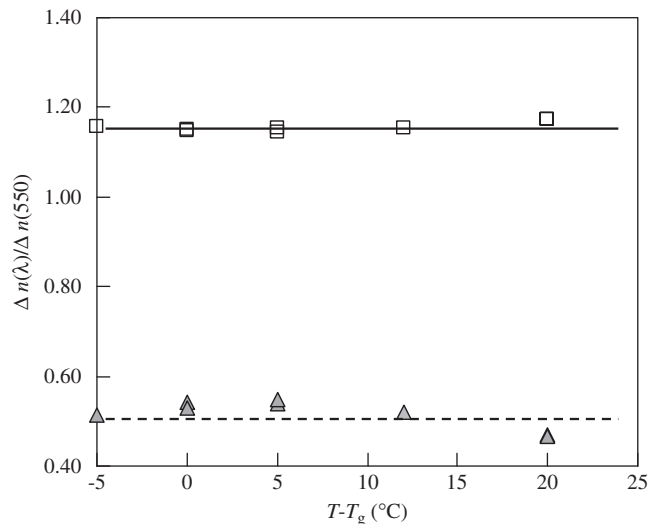
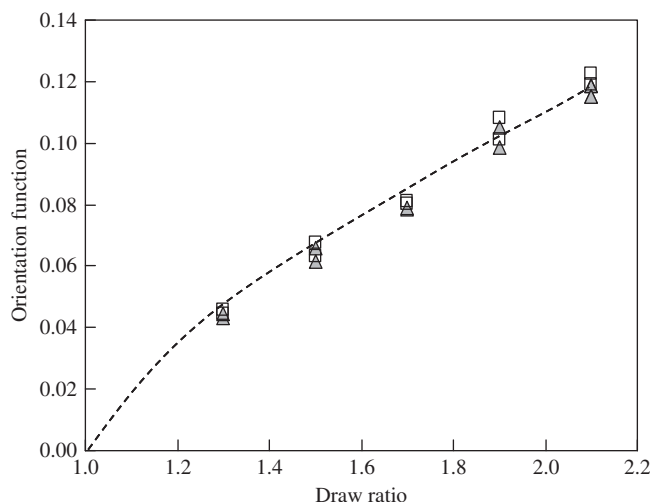
**Figure 22** Normalized birefringence dispersion of co-PC (BPA/BMPF) ($v_p=0.22$, 30 mol% BPA) films stretched at $T_g + 5$ °C as a function of the draw ratio. The triangles and squares indicate the experimental results measured at $\lambda = 450$ and 650 nm, respectively. A full color version of this figure is available at *Polymer Journal* online.

designs of current FPDs, especially for mobile applications. Therefore, the birefringence should be >0.00175 . Co-PCs with volume fractions with near-zero intrinsic birefringence (Figure 17) need much larger orientation functions to generate a birefringence >0.00175 . However, the orientation functions of uniaxially oriented amorphous polymers generally range from 0 to 0.2, depending on the polymer. Polymers with zero intrinsic birefringence cannot be industrialized as retardation films. Therefore, the suitable volume fractions of the co-PCs (BPA/BMPF), which are close to but not equal to zero birefringence points, mostly range from 0.22 to 0.31. The required wide-band properties and large birefringence are satisfied by these co-PCs consisting of BPA and BMPF monomer units. The polymers used for wide-band retardation films are completely different from those necessary for zero birefringence polymers.

Effects of orientation functions on birefringence dispersion

Retardation films are formed by a casting and stretching process. The polymers' molecular orientations are generated during the stretching process. The main factors controlling the orientation functions are the drawing process parameters, with the most effective factors being the drawing ratios and the temperature. Therefore, we examined the influence of orientation functions on the birefringence dispersion by changing the drawing ratios and the temperature.

Figures 22 and 23 illustrate the drawing ratios and the temperature dependence of the birefringence dispersion on the co-PC films consisting of the BPA and BMPF monomer units, respectively. Figures 24 and 25 also illustrate the dependence of the parameter's

**Figure 23** Normalized birefringence dispersion of co-PC (BPA/BMPF) ($v_p=0.22$, 30 mol% BPA) films stretched at a draw ratio of 1.5 as a function of the draw temperature. The triangles and squares indicate experimental results measured at $\lambda = 450$ and 650 nm, respectively. A full color version of this figure is available at *Polymer Journal* online.**Figure 24** Orientation functions of co-PC (BPA/BMPF) ($v_p=0.22$, 30 mol% BPA) films stretched at $T_g + 5$ °C as a function of the draw ratio. The triangles and squares indicate the BPA and BMPF orientation functions, respectively. A full color version of this figure is available at *Polymer Journal* online.

effects on the orientation functions on the co-PCs. The birefringence dispersion of the co-PC films is found to be constant with respect to the two stretching parameters. The orientation functions of the BPA and BMPF monomer units had the same values under any stretching parameters. The constancy of the birefringence dispersion is ascribed to the fact that two orientation functions always indicate the same values. The reason why the dispersions are constant for any stretching parameter can be explained by equation (18). In that equation, f can be eliminated because the orientation functions of each component are approximately equal.

The independence of the birefringence dispersion from the stretching parameters may cause the two following features of these copolymers: (1) these co-PCs comprise a random sequence of

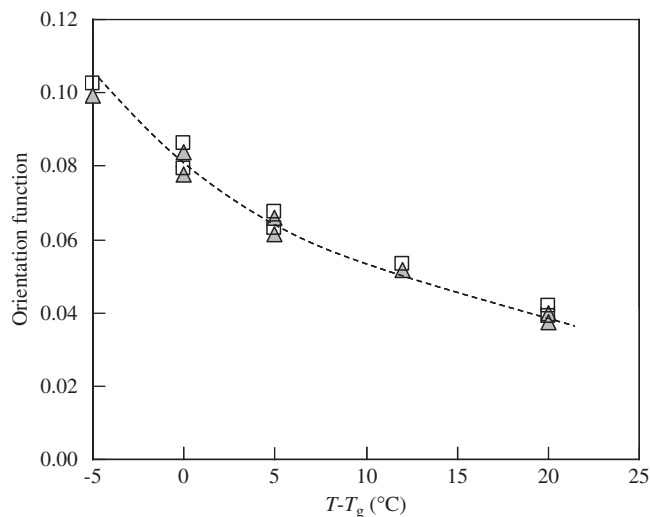


Figure 25 Orientation functions of co-PC (BPA/BMPF) ($v_p=0.22$, 30 mol%BPA) films as a function of stretching temperature at a draw ratio of 1.5. The triangles and squares indicate the BPA and BMPF orientation functions, respectively. A full color version of this figure is available at *Polymer Journal* online.

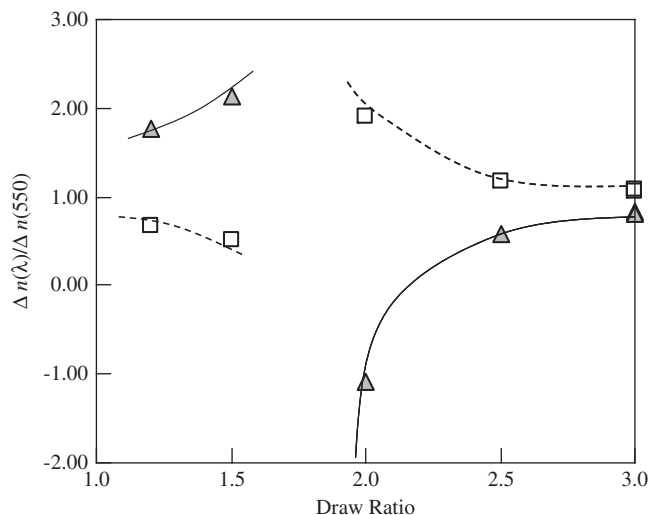


Figure 27 Normalized birefringence dispersion of the uniaxially oriented PPO/PS blend films at 25.6 wt% PPO and at $T_g + 15$ degree C as a function of the draw ratio. The triangles and squares indicate the normalized dispersion values measured at $\lambda=450$ and 650 nm, respectively. A full color version of this figure is available at *Polymer Journal* online.

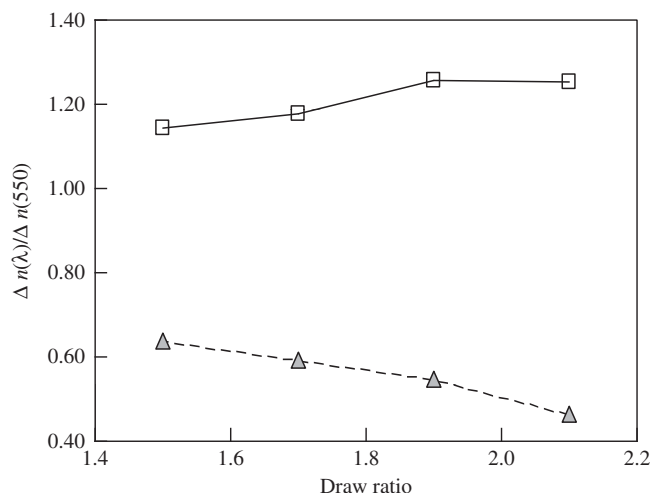


Figure 26 Normalized birefringence dispersion of co-PC (BPA/SPI) (22.4mol% SPI) films stretched at 230 °C as a function of the draw ratio. The triangles and squares indicate experimental results measured at $\lambda=450$ and 650 nm, respectively. A full color version of this figure is available at *Polymer Journal* online.

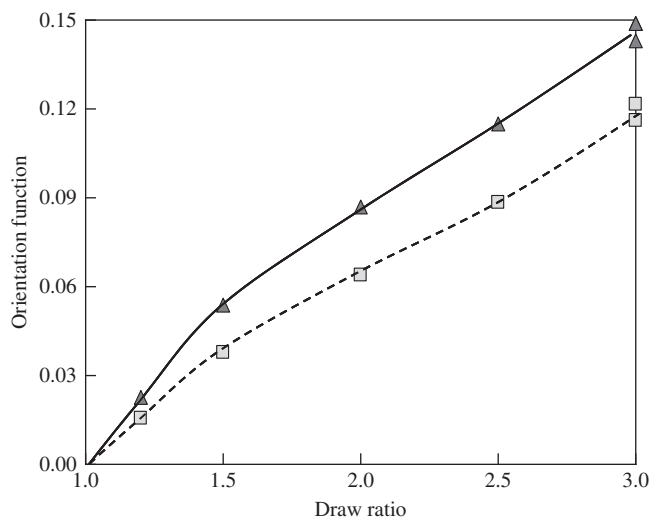


Figure 28 Orientation functions of the uniaxially oriented PPO/PS blend films at 25.6 wt% PPO and at $T_g + 15$ °C as a function of the draw ratio. The triangles and squares represent the orientation functions of PPO and PS, respectively. A full color version of this figure is available at *Polymer Journal* online.

monomer units and (2) the intrinsic birefringence for each monomer unit is constant for all stretching parameters.

Figure 26 illustrates the dependence of birefringence dispersion on the drawing ratio for the BPA and SPI co-PC films. The birefringence dispersion varies with the drawing ratio. We have already reported that the birefringence dispersion of BPA homopolymer films is constant under any stretching parameters for an ordinary production process. Therefore, the change in birefringence dispersion is assumed to be induced by the SPI monomer units. Either the orientation functions of the SPI monomer units may change independently of those of the BPA monomer units or the intrinsic birefringence may vary depending on the stretching parameters.

Figure 27 illustrates the dependence of birefringence dispersion on the drawing ratio for the PS/PPO blend films. Figure 28 illustrates the orientation functions of the PS/PPO films as a function of the drawing ratio. These two orientation functions change independently of each other, with completely different results than those found when examining the co-PC (BPA/BMPF) films. The dispersion change can be explained by the orientation function change according to equation (17). We have also previously demonstrated that the birefringence dispersion changes depending on the drawing temperature.²¹ Therefore, these results show that the birefringence dispersion of the PS/PPO films changes depending on the stretching parameters. Our experimental results are also supported by those of Lefebvre *et al.*,²⁸ who reported similar results for PS/PPO films. Furthermore, our previous

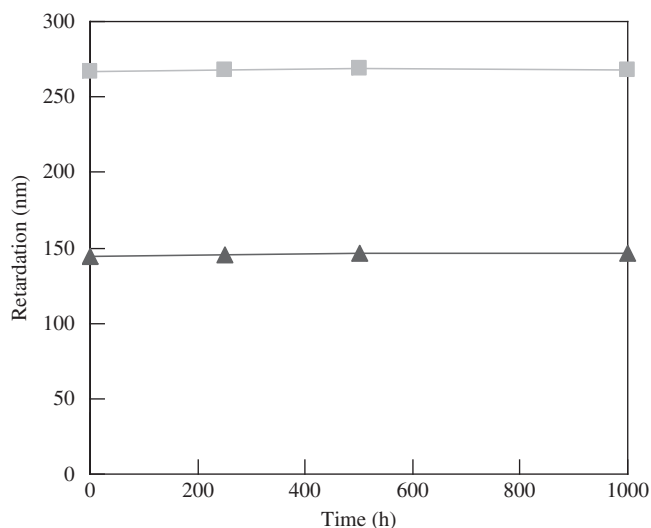


Figure 29 Durability test results of the uniaxially oriented co-PC (BPA/BMPF) films on retardation at 80 °C for 1000 h. The triangles and squares represent films containing 33 and 36 mol% BPA, respectively. A full color version of this figure is available at *Polymer Journal* online.

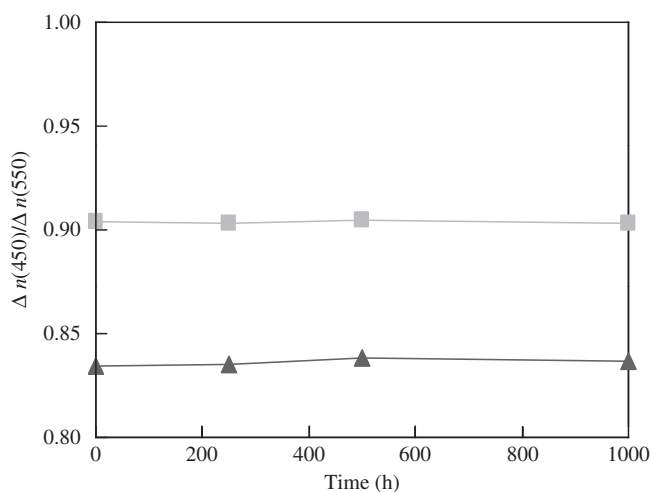


Figure 30 Durability test results of the uniaxially oriented co-PC (BPA/BMPF) films regarding normalized birefringence dispersion at 80 °C at 1000 h. The triangles and the squares represent polymer contents of 33 and 36 mol% BPA monomer units, respectively. A full color version of this figure is available at *Polymer Journal* online.

results have demonstrated that the birefringence dispersion can also be controlled using the PS/PPO blend ratio,²⁰ which can be explained based on equation (17). However, the birefringence dispersion of the PS and PPO homopolymer films has been found to be independently of the stretching parameter.²¹ These results can be explained by our theoretical study, which was discussed in the previous section.

In conclusion, we found two cases where the birefringence dispersion depends on the stretching parameters: in one, the birefringence dispersion is constant, and in the second, it is variable. The variation of the birefringence dispersion in the second case must be controlled by the stretching parameters during the production process. However, this control may not be realistic for industrialization because many other

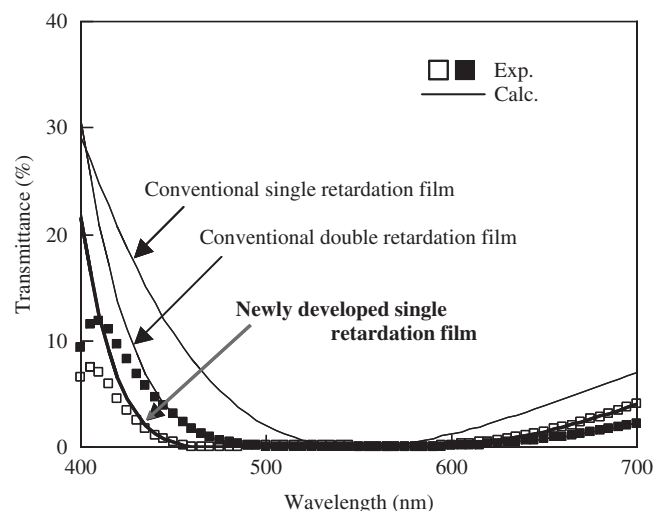


Figure 31 Transmission spectra of circular polarizing films using the equivalent transmissive optical system shown in Figure 14. The newly developed single and conventional retardation films consisted of BPA/BMPF co-PC (BPA/BMPF) ($v_p = 0.24$) and BPA homopolymers, respectively. A full color version of this figure is available at *Polymer Journal* online.

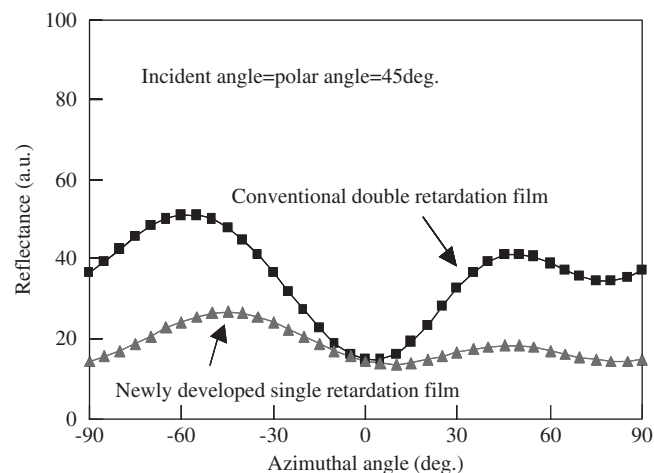


Figure 32 Reflective viewing-angle properties of circular polarizing films measured in the optical configurations shown in Figure 15. The newly developed single and conventional retardation films consisted of BPA/BMPF co-PC (BPA/BMPF) ($v_p = 0.24$) and BPA homopolymers, respectively. A full color version of this figure is available at *Polymer Journal* online.

control parameters are needed to obtain high-quality retardation films during the general production process. Therefore, a constant birefringence dispersion under stretching parameters is optimal. We believe that the BPA and BMPF co-PC film is better than other polymers under these conditions.

Durability

Figures 29 and 30 show the durability test results for the retardation films consisting of BPA and BMPF co-PC (33 and 36 mol% BPA) at 80 °C and 1000 h. The films demonstrate sufficient thermal stability of the retardation and birefringence dispersion for practical applications.

The high T_g of these co-PCs (225–229 °C)²³ is one of the reasons for their high durability.

Optical performance

Figures 31 and 32 show the transmission spectra of circular polarizing films on the equivalent transmissive optical system (see Figures 13 and 14) and the viewing angle reflectance properties of those films, respectively. In the transmission spectra, the circular polarizing film made from the new single wide-band retardation film (the BPA and BMPF co-PC) demonstrates much wider polarization properties than the conventional single retardation film consisting of BPA homopolymer. The new single polarizer also exhibits equal or wider polarization properties, depending on the wavelength range, than does the conventional double-layered retardation film made of BPA-PC, the optical configurations of which are illustrated in Figure 14. These results confirm that our newly developed single retardation film represents a practical, single wide-band retardation film.

Our single retardation film system also has wider viewing angle properties than the conventional double-layered film system (Figure 32). The difference in viewing angle properties is ascribed to the optical film configurations. In the double-layered system, a designed angle of two slow axes in the retardation films is critical to its ability to obtain wide-band birefringence dispersion properties. However, the effective angle of two axes changes largely with the angles of incident light. Therefore, the narrow viewing angle properties of the double-layered system are mainly caused by a gap between the effective angle and the designed angle. The single retardation film system does not have that gap because the wide-band properties are obtained from the molecular structure rather than the optical configuration.

CONCLUSIONS

The following conclusions were derived from the development of the new wide-band retardation films developed on the basis of BDC theory:

1. The new molecular design method using mixtures of positive and negative monomer units has established and enabled us to control the birefringence dispersion of polymer films. Controlling the ratio of positive to negative monomer units in a copolymer or blend polymer is proved to be essential. The wide-band properties of birefringence dispersion only eventuate in the narrow volume fraction range close to, but not at, the zero birefringence point. The molecular designed polymer in the narrow range must generate birefringence large enough for practical applications.
2. The relationship between the orientation functions and the birefringence dispersion of the copolymers and blend polymers show that there are two types of films, one with constant birefringence dispersion and one with birefringence that varies depending on the stretching parameters. Discovering a new co-PC with constant birefringence properties has enabled us to produce stable films for use as novel wide-band retardation films.
3. The newly developed wide-band retardation films, consisting of BPA and BMPF co-PC, satisfy all of the requirements of retardation films, including not only the wide-band properties of birefringence, but also such properties as sufficiently large birefringence, thermal stability and other practical specifications.

The novel wide-band retardation films designed on the basis of BDC theory have been industrialized by the Teijin Group and have been widely used in FPDs, such as LCDs and OLEDs, thereby contributing to improved display images.

ACKNOWLEDGEMENTS

We are grateful to Professor Tatsuo Uchida (Sendai National College of Technology, Professor Emeritus of Tohoku University), Professor Tetsuya Miyashita from the Tohoku Institute of Technology and Assistant Professor Takahiro Ishinabe from Tohoku University for their insightful advice and guidance on the research cited in this article. The development of wide-band retardation films was successful because of the efforts of many people at Teijin Ltd. and Teijin Chemicals Ltd, and we appreciate their support.

- 1 Wada, H., Wada, S. & Iijima, C. Liquid crystal display device and method of fabrication, US Patent. 4844569 (1989).
- 2 Ishinabe, T., Miyashita, T. & Uchida, T. Wide-viewing-angle polarizer with a large wavelength range. *Jpn. J. Appl. Phys.* **41**, 4553–4558 (2002).
- 3 Uchiyama, A., Ishinabe, T., Miyashita, T., Uchida, T., Ono, Y. & Ikeda, Y. Novel design method using birefringence dispersion control of retardation films for a high contrast LCD in wide viewing angle range. *Proc. 11th Int. Display Workshops* 647–650 (2004).
- 4 Fujimura, Y., Nagatuka, T., Yoshimi, H. & Shimomura, T. Optical properties of retardation films for STN-LCDs. *Soc. Inform. Display Dig.* 739 (1991).
- 5 Mori, H., Itoh, Y., Nishiura, Y., Nakamura, T. & Shinagawa, Y. Performance of a novel optical compensation film based on negative birefringence of discotic compound for wide-viewing-angle twisted-nematic liquid-crystal displays. *Jpn. J. Appl. Phys.* **36**, 143–147 (1997).
- 6 Toko, Y., Sugiyama, T., Katoh, K., Iimura, Y. & Kobayashi, S. Amorphous twisted nematic-liquid-crystal displays fabricated by nonrubbing showing wide and uniform viewing-angle characteristics accompanying excellent voltage holding ratios. *J. Appl. Phys.* **74**, 2071–2076 (1993).
- 7 Pancharatnam, S. Achromatic combination of birefringent plates. *Proc. Indian Acad. Sci.* **A41**, 130–136 (1955).
- 8 Uchiyama, A. & Kushida, T. Phase difference film and optical device using it, International Patent. W000/26705 (2000).
- 9 Uchiyama, A. & Yatabe, T. Wide-band retardation films with reverse wavelength dispersion. *Proc. 7th Int. Display Workshops* 407–410 (2000).
- 10 Uchiyama, A., Ono, Y., Ikeda, Y., Kawada, I. & Yatabe, T. Recent progress in optical retardation films for FPDs. *Proc. 9th Int. Display Workshops* 493–496 (2002).
- 11 Uchiyama, A., Ishinabe, T., Miyashita, T., Uchida, T., Ono, Y. & Ikeda, Y. Novel design method of retardation films for a high contrast LCD in wide viewing angle range. *20th International Liquid Crystal Conference Book of Abstracts* 61 (2004).
- 12 Yeh, P. & Gu, C. in *Optics of Liquid Crystal Displays* (ed. Goodman, J. W.) Ch. 9 357–389 (Wiley Inter-Science, New York, 1999).
- 13 Hibi, S., Maeda, M., Takeuchi, M., Nomura, S., Shibata, Y., Shibata, Y. & Kawai, H. Effects of crystallinity on orientation behavior in uniaxially stretched polyvinyl alcohol. *Sen-I Gakkaishi* **27**, 20–29 (1971).
- 14 Hibi, S., Maeda, M., Indo, T., Mizuno, M., Nomura, S. & Kawai, H. Orientation evaluation of crystalline phase and noncrystalline phase of orthogonal-biaxially stretching polyvinyl alcohol. *Sen-I Gakkaishi* **28**, 246–258 (1972).
- 15 Stein, R. S. & Wilkes, G. L. in *Structure and Properties of Oriented Polymers* (ed. Ward, I. M.) Ch. 3 57–70 (Applied Science Publishers, London, 1975).
- 16 Holliday, L. & Ward, I. M. in *Structure and Properties of Oriented Polymers* (ed. Ward, I. M.) Ch. 1 1–35 (Applied Science Publishers, London, 1975).
- 17 Saito, H. & Inoue, T. Chain orientation and intrinsic anisotropy in birefringence-free polymer blends. *J. Polym. Sci. Part B Polym. Phys.* **25**, 1629–1636 (1987).
- 18 Uchiyama, A., Ikeda, Y. & Yatabe, T. Effect of three-dimensional refractive index change on birefringence dispersion of oriented bisphenol A polycarbonate films. *Kobunshi Ronbunshu* **60**, 38–44 (2003).
- 19 Aspnes, D. E. Optical properties of thin films. *Thin Solid Films* **89**, 249–262 (1982).
- 20 Uchiyama, A. & Yatabe, T. Analysis of extraordinary birefringence dispersion of uniaxially oriented poly(2,6-dimethyl-1,4-phenylene oxide)/atactic polystyrene blend films. *Jpn. J. Appl. Phys.* **42**, 3503–3507 (2003).
- 21 Uchiyama, A. & Yatabe, T. Control of birefringence dispersion of uniaxially oriented poly(2,6-dimethyl-1,4-phenylene oxide)/atactic polystyrene blend films by changing the stretching parameters. *Jpn. J. Appl. Phys.* **42**, 5665–5669 (2003).
- 22 Inoue, T., Kuwada, S., Ryu, D. & Osaki, K. Effect of wavelength on strain-induced birefringence of polymers. *Polym. J.* **30**, 929–934 (1998).
- 23 Uchiyama, A. & Yatabe, T. Molecular orientation of aromatic polycarbonate containing fluoreneside chain by polarized infrared spectroscopy and birefringence analysis. *J. Polym. Sci. Part B Polym. Phys.* **41**, 1554–1562 (2002).
- 24 Uchiyama, A. & Yatabe, T. Control of wavelength dispersion of birefringence for oriented copolycarbonate films containing positive and negative birefringent units. *Jpn. J. Appl. Phys.* **42**, 6941–6945 (2003).
- 25 Fukazawa, T. & Fujita, Y. Polarization modulated transmission spectro-ellipsometry. *Rev. Sci. Instrum.* **67**, 1951–1955 (1996).
- 26 Read, B. E. in *Structure and Properties of Oriented Polymers* (ed. Ward, I. M.) Ch. 4 150–184 (Applied Science Publishers, London, 1975).
- 27 Uchiyama, A., Ono, Y., Ikeda, Y., Shuto, H. & Yahata, K. Development of copolycarbonate optical film using birefringence dispersion control. *Polym. Preprints Jpn.* **60**, 25–27 (2011).
- 28 Lefebvre, D., Jasse, B. & Monnerie, L. Fourier transform infra-red study of uniaxially oriented poly(2,6-dimethyl-1,4-phenylene oxide)-atactic polystyrene blends. *Polym* **22**, 1616–1620 (1981).



Dr Akihiko Uchiyama was born in Tokyo, Japan in 1967. He received his master degree of Engineering in 1992 from Chiba University and his Doctoral degree of Engineering in 2004 from Tohoku University under the supervision of Professor Tatsuo Uchida. He joined Teijin Ltd. (Japan) in 1992 and started his R&D at Advanced Thin Film Research Laboratories. Since then he has been mainly engaged in the R&D of photonics materials such as liquid crystals and functional optical films for flat panel displays (1992–2008). He is currently a senior technical expert of Teijin group and developing bio-based polymers and their applications at High Performance Biomaterials Project. His recent research interests include functional polymer materials and bio-based polymers. He was a recipient of The Award of the Society of Polymer Science, Japan (2010).



Yuhei Ono was born in Kagawa Prefecture, Japan in 1973. He received his master degree of Engineering in 1999 from Nagoya Institute of Technology. He joined Teijin Ltd. in 1999. He was engaged in the engineering R&D in 1999 and was transferred to the R&D division of new business development group in 2000. Since then he has researched optical films for liquid crystal displays. He is currently a member of High Performance Biomaterials Project, and researching highly functional films of biomaterials. He was a recipient of The Award of the Society of Polymer Science, Japan (2010).



Dr Yoshinori Ikeda was born in Ehime Prefecture, Japan in 1975. He received his master degree in 1998 from Kyushu University and his Doctoral degree of Engineering in 2010 from Tokyo University of Agriculture and Technology under the supervision of Professor Toshiyuki Watanabe. He joined Teijin Ltd. in 1998. Since then he has been mainly engaged in the R&D of electronics materials such as optical recording media (1998–2001), optical films for liquid crystal displays (2001–2010). He is currently a chief at Integrative Technology Research Laboratories. His recent research interests include printable semiconductor materials and their applications. He was a recipient of The Award of the Society of Polymer Science, Japan (2010).



Hiroshi Shuto was born in Osaka Prefecture, Japan in 1969. He received his master degree of Engineering in 1994 from Kyoto Institute of Technology. He joined Teijin Chemicals Ltd. (Japan) in 1994. Since then he has been mainly engaged in the R&D of polymer materials such as optical recording media (1994–2001), optical films for Liquid Crystal Displays (2001–2004). He is currently an adviser at manufacturing section in Teijin Polycarbonate China Ltd. He was a recipient of The Award of the Society of Polymer Science, Japan (2010).



Kazuo Yahata was born in Tokyo, Japan in 1963. He received his master degree from Tokyo Institute of Technology in 1989. In the same year he joined Teijin Ltd. and started his R&D at New Material Research Laboratories. He was transferred to TF factory in 2000, he was engaged in the R&D of manufacturing optical films for LCD, OLED display and optical recording media. He is currently a manager at third Manufacturing Section Mihara Plant (Teijin Chemicals Ltd). His recent research interests include transparent conductive film for Touch Panel and E-paper. He was a recipient of The Award of the Society of Polymer Science, Japan (2010).